Journal of Reproduction and Development, Vol. 60, No 6, 2014

—Original Article—

Ultrastructure of immature and mature human oocytes after cryotop vitrification

Maria Grazia PALMERINI[1)], Monica ANTINORI[2)], Marta MAIONE[3)], Fabrizio CERUSICO[2)], Caterina VERSACI[2)], Stefania Annarita NOTTOLA[3)], Guido MACCHIARELLI[1)], Mohammad Ali KHALILI[4)] and Severino ANTINORI[2)]

[1)]*Department of Life, Health and Environmental Sciences, University of L'Aquila, L'Aquila, Italy*
[2)]*RAPRUI Day Hospital (International Associated Research Institute for Human Reproduction), Rome, Italy*
[3)]*Department of Anatomy, Histology, Forensic Medicine and Orthopaedics, University La Sapienza, Rome, Italy*
[4)]*Research and Clinical Center for Infertility, Shahid Sadoughi University of Medical Sciences, Yazd, Iran*

Abstract. *In vitro* maturation of vitrified immature germinal vesicle (GV) oocytes is a promising fertility preservation option. We analyzed the ultrastructure of human GV oocytes after Cryotop vitrification (GVv) and compared it with fresh GV (GVc), fresh mature metaphase II (MIIc) and Cryotop-vitrified mature (MIIv) oocytes. By phase contrast microscopy and light microscopy, the oolemmal and cytoplasmic organization of fresh and vitrified oocytes did not show significant changes. GVv oocytes showed significant ultrastructural alterations of the microvilli in 40% of the samples; small vacuoles and occasional large/isolated vacuoles were abnormally present in the ooplasm periphery of 50% of samples. The ultrastructure of nuclei and mitochondria-vesicle (MV) complexes, as well as the distribution and characteristics of cortical granules (CGs), were comparable with those of GVc oocytes. MIIv oocytes showed an abnormal ultrastructure of microvilli in 30% of the samples and isolated large vacuoles in 70% of the samples. MV complexes were normal, but mitochondria-smooth endoplasmic reticulum aggregates appeared to be of reduced size. CGs were normally located under the oolemma but presented abnormalities in distribution and matrix electron density. In conclusion, Cryotop vitrification preserved main oocyte characteristics in the GV and MII stages, even if peculiar ultrastructural alterations appeared in both stages. This study also showed that the GV stage appears more suitable for vitrification than the MII stage, as indicated by the good ultrastructural preservation of important structures that are present only in immature oocytes, like the nucleus and migrating CGs.
Key words: GV stage, Human, Oocyte, Ultrastructure, Vitrification

(**J. Reprod. Dev. 60:** 411–420, 2014)

Among the available cryopreservation techniques for human oocytes [1, 2], vitrification is no longer considered only a promising alternative to conventional slow freezing. Many infants have been conceived after oocyte vitrification with no related adverse obstetric and perinatal outcomes [3, 4]. With respect to slow freezing, several reports evidence higher post-thaw survival and higher fertilization, implantation and pregnancy rates obtained using vitrified oocytes [5–7]. Today, vitrification is widely adopted, even if its superiority over slow freezing in preserving oocyte ultrastructure is still a matter of debate. Two previous reports [8, 9] found significantly higher percentages of normal meiotic spindles and of chromosome alignment in vitrified-warmed oocytes than in frozen-thawed ones, differing from what was reported by another study [10]. Actually, the data available on the matter are not yet exhaustive, mainly as a consequence of the use of different vitrification cryotools. Among cryodevices, the Cryotop seems to give good results [11, 12], but as in the case of all the other open devices, it has been considered to be potentially susceptible to pathogen contamination of samples, as it is directly plunged into liquid nitrogen. To overcome this hypothetical risk, the Cryotop method has also been applied in combination with the use of nitrogen in the vapor phase [13] or liquid nitrogen sterilized by UV [14].

Currently, protocols for oocyte cryopreservation are less effective than those for embryo cryopreservation in assisted reproductive technologies (ARTs) [15]. In particular, mature metaphase II-stage (MII) oocytes can be difficult to cryopreserve mainly because of their large size, as well the high water content, the high degree of cytoplasmic specialization (including cytoskeletal characteristics) and the precise chromosomal arrangement [1]. Cryopreservation of immature germinal vesicle-stage (GV) oocytes could elude some of the above problems, particularly those related to the cryodamage of the spindle and of chromosomes. On the other hand, GV oocytes need to be matured *in vitro*. To date, *in vitro* maturation (IVM) methods have not yet been optimized in humans [16]. In fact, several parameters, such as the culture medium composition, hormonal supplementation and co-culture with granulosa cells [17–19], can alter maturation rates. Recently, attention has also been given to wheter IVM should be performed before or after vitrification [16, 20].

Received: February 24, 2014
Accepted: July 14, 2014
Published online in J-STAGE: August 28, 2014

Correspondence: MG Palmerini (e-mail: mariagrazia.palmerini@univaq.it)

In the present work, since the stage-dependent cryodamage is not well understood in human oocytes, we studied the effects of vitrification using the Cryotop method [21] on the ultrastructural morphology of supernumerary GV oocytes collected from consenting patients, undergoing treatment with ARTs. In order to reveal stage-dependent cryodamage for the first time, the ultrastructure of immature GV-stage oocytes was compared with that of mature MII-stage oocytes. The presence of morphological modifications was evaluated by means of phase contrast microscopy (PCM), light microscopy (LM) and transmission electron microscopy (TEM).

Materials and Methods

Patients

Human GV and MII oocytes were collected from 14 women (mean age 32.07 ± 1.54) undergoing assisted reproduction treatments because of infertility due to tubal factors. All women included in the study provided written informed consent; the clinical study was formally approved by the Ethical Committee of the *International Associated Research Institute for Human Reproduction,* Rome, Italy.

Ovarian stimulation was achieved using a long gonadotropin-releasing hormone agonist (GnRH-A) protocol (Decapeptyl 3.75, Ipsen SpA, Italy) in combination with rFSH (Gonal F, Merck Serono, Rome, Italy) 150 IU per day. Follicular growth was monitored by serum 17β-estradiol measurements and ovarian ultrasonography. Ovulation was induced using 10,000 IU of human chorionic gonadotropin (hCG) (Gonasi HP, AMSA, Italy) when at least 3 follicles with a diameter ≥ of 17 mm were detected and the 17β-estradiol levels corresponded to the number of follicles. Transvaginal ultrasound guided oocyte retrieval was performed 34–36 h later. Only oocytes without any sort of dysmorphisms at PCM examination were used for the experiment and assigned to the groups of GV oocytes (with an evident nucleus) or MII oocytes (with an extruded polar body 1, PB1).

Oocytes were fixed 3–4 h after sampling (fresh control GV [GVc] and mature metaphase II [MIIc] oocytes) or frozen using vitrification 3 h after retrieval. Vitrified-warmed oocytes (GVv and MIIv) were cultured for 2 more hours before fixation.

Oocyte vitrification and warming

Oocyte vitrification and warming procedures were performed as previously described [21]. In brief, after retrieval, decumulated GV and MII oocytes were incubated in equilibration solution containing 7.5% ethylene glycol (EG) (Sigma-Aldrich, Steinheim, Germany) and 7.5% dimethyl dulfoxide (DMSO) (Sigma-Aldrich) in Ham´s F-10 medium supplemented with 20% Serum Substitute Supplement (SSS, Irvine Scientific, Santa Ana, CA, USA). Equilibration was performed for 5–15 min (according to the time needed for the re-expansion of the oocyte) at room temperature. After an initial shrinkage and recovery, oocytes were subsequently transferred into the vitrification solution (15% EG, 15% DMSO and 0.5 M Sucrose) (Merck, Darmstadt, Germany) for less than 60 sec at room temperature and positioned on a Cryotop tip (Kitazato, Tokyo, Japan). The device was immediately plunged into liquid nitrogen for storage. Oocyte warming was performed by placing the Cryotop tip once into the thawing solution (1 M sucrose), for less than 60 sec at 37 C and then twice into the dilution solution (0.5 M sucrose) for 3 min. Warmed oocytes were placed 4–5 times into a washing solution (Ham's F-10 plus 20% serum) and then positioned in 5% CO_2 in an incubator at 37 C for 2 h.

Electron microscopy

A total of 21 GV (9 GVc and 12 GVv) and 24 MII (10 MIIc and 14 MIIv) oocytes were included in this study. Oocytes were fixed and processed for TEM analysis as previously described [22]. Oocyte fixation was performed in 1.5% glutaraldehyde (SIC, Rome, Italy) in a phosphate buffered saline (PBS) solution. After fixation for at least 2 days at 4 C, the samples were rinsed in PBS, postfixed with 1% osmium tetroxide (Agar Scientific, Stansted, UK) in PBS and rinsed again in PBS. Oocytes were then embedded in small blocks of 1% agar of about 5 × 5 × 1 mm in size, dehydrated in an ascending series of ethanol (Carlo Erba Reagenti, Milan, Italy), immersed in propylene oxide (BDH Italia, Milan, Italy) for solvent substitution, embedded in epoxy resin EMbed-812 (Electron Microscopy Sciences, Hatfield, PA, USA) and sectioned by means of a Reichert-Jung Ultracut E ultramicrotome. Semithin sections (1 mm thick) were stained with Toluidine Blue, examined using LM (Zeiss Axioskop) and photographed using a digital camera (Leica DFC230). Ultrathin sections (60–80 nm) were cut with a diamond knife, mounted on copper grids and contrasted with saturated uranyl acetate and lead citrate (SIC, Rome, Italy). They were examined and photographed using Zeiss EM10 and Philips TEM CM100 Electron Microscopes operating at 80 KV.

According to previous papers [1, 23–25], the following parameters were evaluated by LM and TEM and taken into consideration for qualitative assessment of the ultrastructural preservation of oocytes: general features (shape and dimensions); integrity of the oolemma; microtopography and type and quality of the organelles; *zona pellucida* (ZP) texture; appearance of the perivitelline space (PVS) (width, presence of fragments, presence and characteristics of the PB1); characteristics of the nucleus, chromatin and nuclear envelope; and presence and extent of cytoplasmic vacuolization. Regarding the selection and classification of vacuoles by TEM, we evaluated the electron-lucent vacuoles with a diameter of at least 0.2 μm (at a magnification of 1200 × during TEM observation), i.e., corresponding to the size of vacuoles detectable by LM at a magnification of 400 ×. In addition, we considered the vacuoles with a diameter < 1.5 μm as "small vacuoles" and those with a diameter > 1.5 μm as "large vacuoles."

Morphometric analysis

The ImageJ software (http://rsbweb.nih.gov/ij/; last access June 4, 2014) was used to measure the dimensions of mitochondria, cortical granules (CGs) and vacuoles on low-magnification TEM micrographs of an equatorial section. For each experimental group, at least three oocytes were selected for statistical analysis.

Statistical analysis

All data were expressed as means ± standard deviation (SD) and compared with the unpaired *t*-test (GraphPad InStat). Differences in values were considered significant if $P < 0.05$.

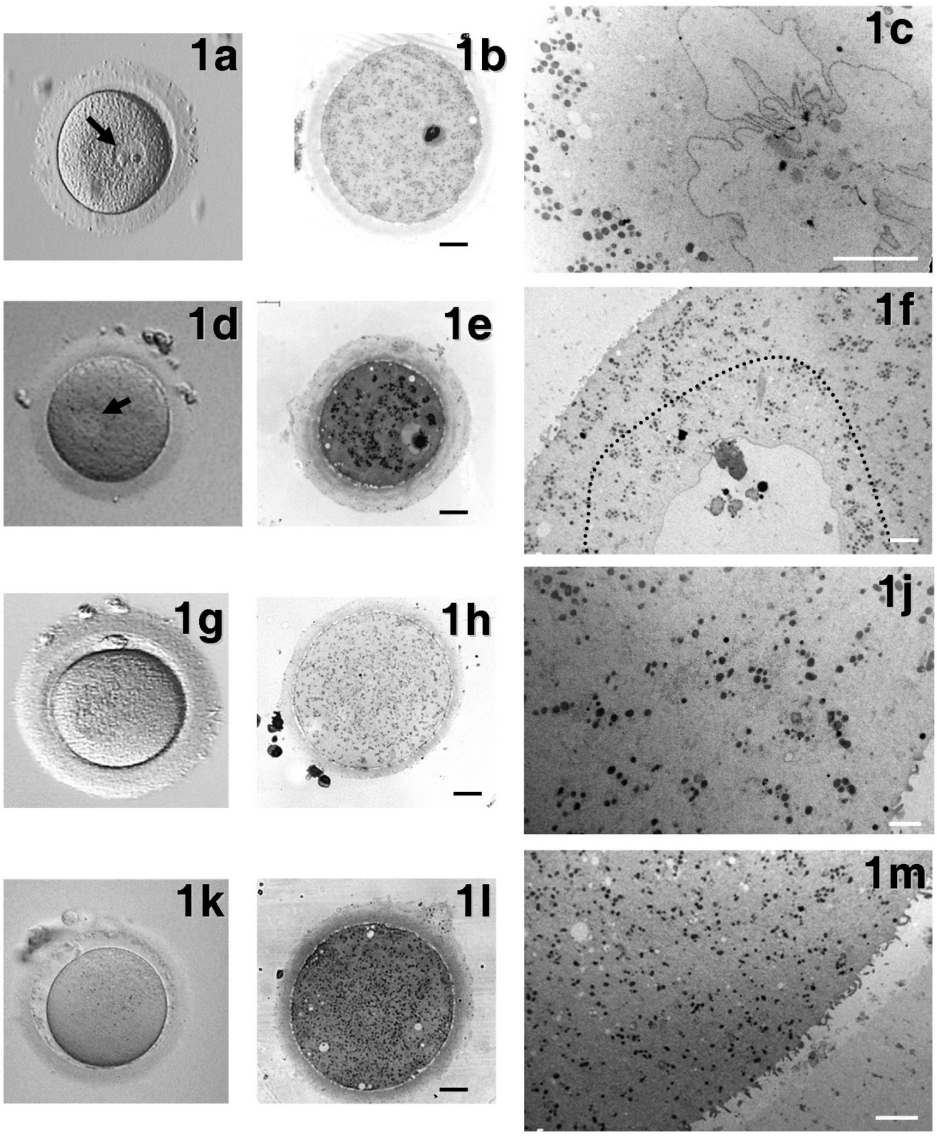

Fig. 1. General morphology and organelle microtopography in immature and mature human oocytes, either fresh or vitrified by the Cryotop method. Representative phase contrast microscopy (PCM) (a, d, g, k) (40 × magnification), light microscopy (LM) (b, e, h, l) (bars: 20 µm) and transmission electron microscopy (TEM) (c, f, j, m) (bars: 5 µm) images of GVc (a–c), GVv (d–f), MIIc (g–j) and MIIv (k–m) oocytes are shown. Arrows in Figs. 1a and 1d indicate the nucleus. The dotted line in Fig. 1f delimitates the physiological presence of small vacuoles in the ooplasm surrounding the nucleus.

Results

All GV and MII oocytes subjected to Cryotop vitrification survived after warming. By PCM, they showed good quality, as evidenced by their regular shape and the integrity of ZP, oolemma and PVS. All fresh controls exhibited a good morphological appearance by PCM.

GV oocytes

Fresh controls (GVc): PCM evaluation revealed that all GVc oocytes were normal, with a round shape, a compact ZP surrounding a homogeneous ooplasm and a visible nucleus eccentrically located (Fig. 1a). By LM, the ooplasm appeared rich in organelles (Fig. 1b), which were sometimes more abundant in the area surrounding the nucleus. By TEM, the remnants of corona cell prolongations were found in the ZP and on the oolemma. A continuous layer of thin and long microvilli covered the oocyte surface (Fig. 2a). Spherical CGs (medium diameter ± SD: 0.348 ± 0.113 µm, Table 1) were randomly distributed in the ooplasm and only occasionally present in the cortex (Fig. 3a). The CG electron density ranged from light to dark, but dark CGs were the most represented (Fig. 3a).

TEM showed the presence of dense ellipsoidal/spheroid mitochondria (medium diameter ± SD: 0.405 ± 0.107 µm, Table 1), isolated tubules of smooth endoplasmic reticulum (SER), a few Golgi complexes (Figs. 1c, 2a, 3a) and lysosomes. Numerous small

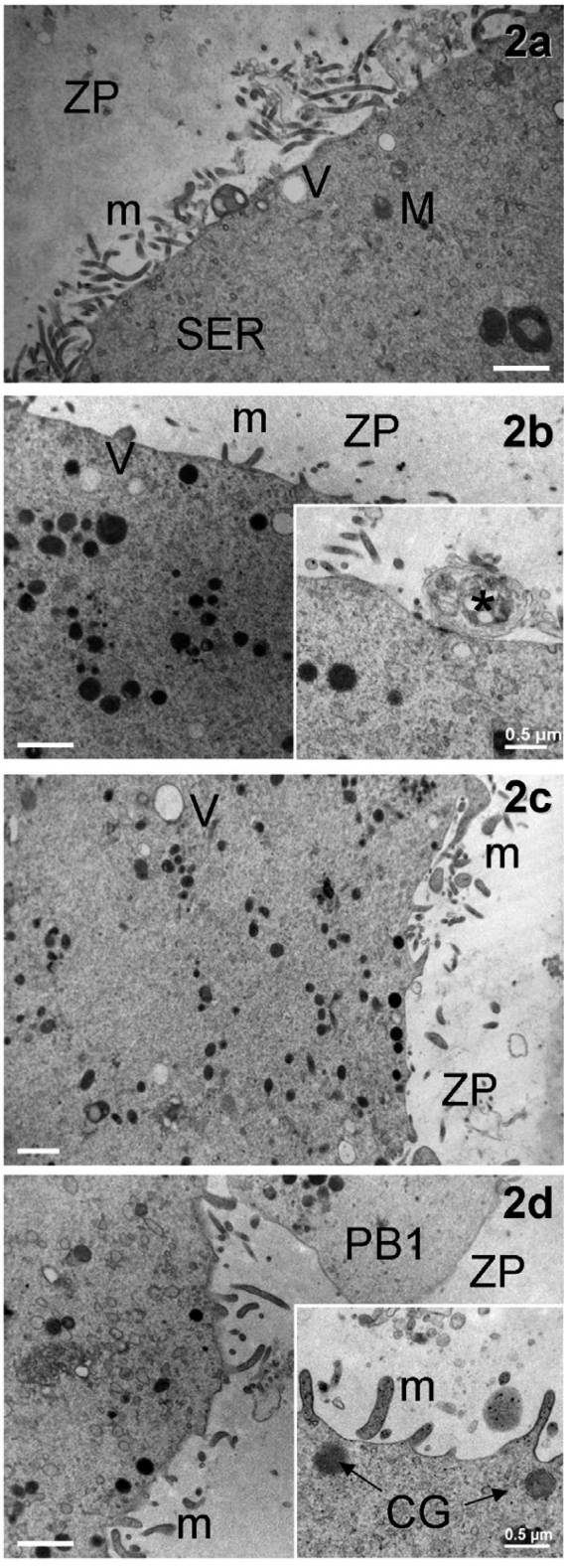

Fig. 2.

mitochondria-vesicle (MV) complexes were identified in the cortex and subcortex (inset in Fig. 3a). Underdeveloped M-SER aggregates were occasionally observed.

Numerous vacuoles, small and empty (medium diameter ± SD: 0.975 ± 0.113 µm, Table 1), were found mainly in the region surrounding the nucleus (Fig. 1c). An electron-dense nuclear membrane provided with pores surrounded a spherical nucleus with one or a few dense nucleolar bodies. Small patches of condensed chromatin were sometimes visible near the nucleolar bodies (Fig. 1c).

Vitrified-warmed GV (GVv): GVv oocytes showed a regular round shape by PCM examination, with the nucleus clearly visible and usually located at the periphery of the ooplasm (Fig. 1d). Semithin sections analyzed by LM evidenced a physiologic distribution of organelles scattered in a homogeneous ooplasm. The ZP appeared continuous and well preserved (Fig. 1e). Short and small microvilli were irregularly distributed on the oolemma of 40% of GVv oocytes and projected into the PVS towards the ZP, as shown by TEM analysis (Fig. 1f). Under the ZP, several corona cell endings, forming focal cell contacts−small desmosomes or gap junctions−with the oolemma, were evidenced (Fig. 2b, inset). CGs (medium diameter ± SD: 0.409 ± 0.680 µm, Table 1) were found scattered in the ooplasm (Fig. 3b). They presented a round shape and a variable electron-dense content, as in the fresh counterpart (Figs. 3a, 3b). In close proximity of CGs, Golgi complexes were often visible with stacks of flattened sacs and small secretory vesicles (Fig. 3b). Mitochondria were abundant, often clustered and round or slightly ovoid in shape (medium diameter ± SD: 0.450 ± 0.122 µm, Table 1) (Figs. 1f, 2b). At higher magnification, mitochondria were dark (electron dense) with a continuous membrane and a few peripheral or transversal *cristae* (Fig. 3b). In some cases, clear vacuoles were present inside the mitochondrial matrix (Fig. 3b). SER tubules were often found in the ooplasm, together with rare lipid droplets. Isolated or grouped MV complexes were occasionally identified in the ooplasm (Fig. 3b, inset).

Some physiologic vacuolization, mainly represented by small, empty membrane-bounded vacuoles (medium diameter ± SD: 0.622 ± 0.494 µm, Table 1), was observed around the nucleus (Fig. 1f, ooplasm delimited by the dotted line). In addition, abnormally small and occasionally large isolated vacuoles were found in the periphery of the ooplasm in 50% of the GVv oocytes (Figs. 1e, 1f, 2b). The concomitant presence of vacuoles and altered microvilli in the same oocyte was found in 25% of samples.

The nucleus was normally located (Figs. 1e, 1f) and contained euchromatin fibrils finely dispersed throughout the nucleoplasm with the exception of a few dense and round nucleolar bodies, which

Fig. 2. General appearance of the cortical region in immature and mature human oocytes, either fresh or vitrified by the Cryotop method. Micrographs of GVc (a), GVv (b), MIIc (c) and MIIv (d) oocytes showing the general distribution and length of microvilli, as seen by TEM (bars: 1 µm). In d, a section of the PB1 is also included. The inset in b shows a corona cell ending forming a focal cell contact (*)−small desmosome or gap junction−with the oolemma (bar: 0.2 µm). The inset in d magnifies clear microvilli with an electron-dense membrane (bar: 0.5 µm). V = vacuoles, m = microvilli, M = mitochondria, SER = smooth endoplasmic reticulum, CG = cortical granules, ZP = *zona pellucida*, and PB1 = 1st polar body.

Table 1. Medium diameter ± standard deviation (SD) of cortical granules, mitochondria and vacuoles in immature and mature human oocytes before and after Cryotop vitrification

	GVc	GVv	MIIc	MIIv
Cortical granules (µm)	0.348 ± 0.113	0.409 ± 0.680	0.286 ± 0.098	0.341 ± 0.065
Mitochondria (µm)	0.405 ± 0.107	0.450 ± 0.122	0.368 ± 0.084	0.359 ± 0.084
Small/large Vacuoles (µm)	0.975 ± 0.113	0.622 ± 0.494	0.686 ± 0.745	1.086 ± 1.049

Approximately 10 to 50 cortical granules, 70 to 150 mitochondria and 50 to 100 vacuoles were measured in low magnification TEM micrographs from at least three different oocytes per stage. Statistical analysis, performed within the same nuclear stage for comparison between control and vitrified oocytes, did not show significant differences (P > 0.05).

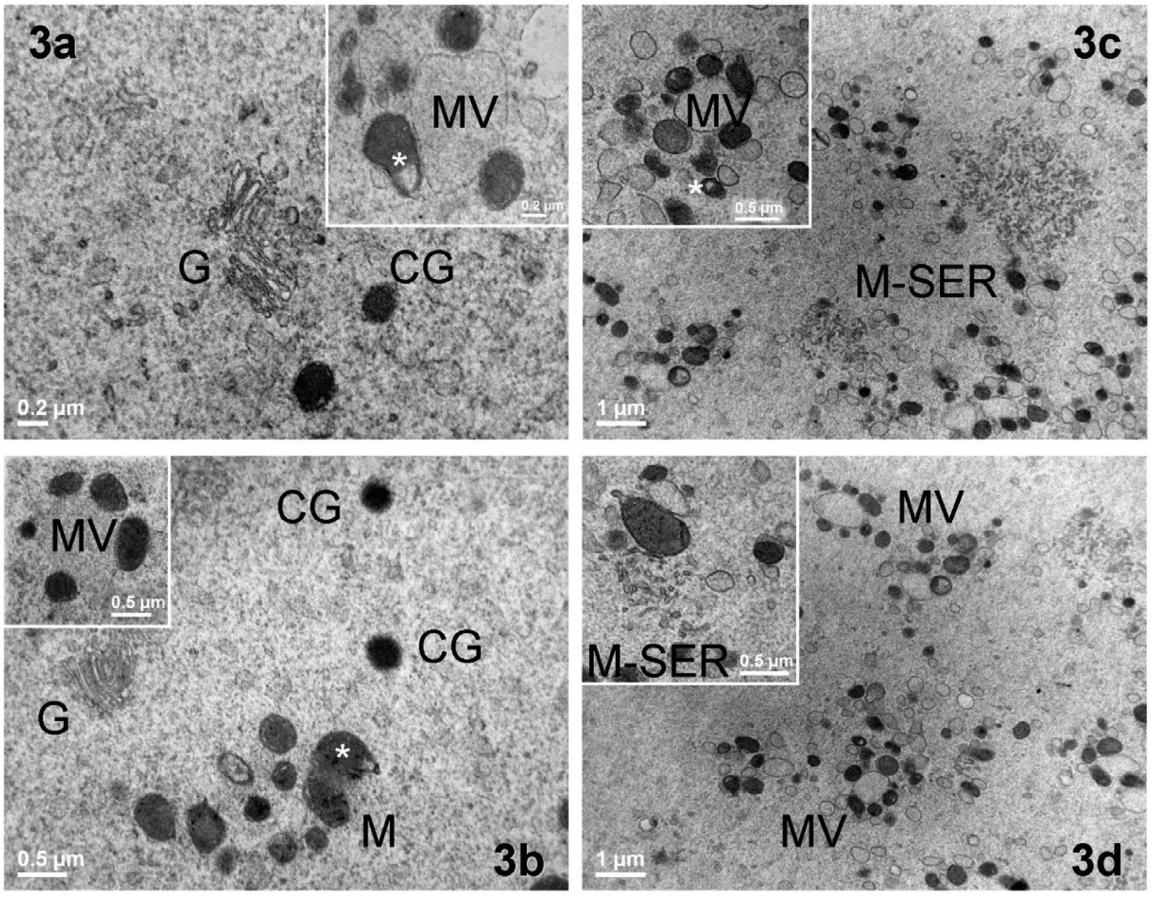

Fig. 3. Ultrastructure and distribution of oocyte organelles in immature and mature human oocytes, either fresh or vitrified by the Cryotop method. Representative TEM micrographs of intracellular organelles in GVc (a), GVv (b), MIIc (c) and MIIv (d) oocytes. Clusters of mitochondria (M), also containing a clear vacuole (white asterisk), Golgi complexes (G) and cortical granules (CG), are shown in the inner ooplasm (bar: 0.5 µm). *Insets* in a, b and c represent a mitochondria-vesicle (MV) complex (bar: 0.5 µm). In MIIv oocytes, clusters of MV complexes are present (bar: 1 µm). The inset in d evidences a mitochondria-SER aggregate (M-SER) (bar: 0.5 µm).

were associated with condensed heterochromatin (Fig. 4a). At higher magnification, the nuclear envelope was slightly undulated and perforated by numerous normal nuclear pores (Fig. 4b).

MII oocytes

Fresh controls (MIIc): MIIc oocytes showed a round shape, a homogeneous ooplasm and a visible PB1 by PCM examination (Fig. 1g). LM revealed the presence of a continuous ZP, a narrow PVS and abundant cytoplasmic organelles, often in clusters (Fig. 1h). Ultrastructural analysis by TEM revealed a normal distribution of organelles and an oolemma provided with numerous long and thin microvilli projecting into the PVS. A continuous layer of electron-dense round CGs (medium diameter ± SD: 0.286 ± 0.098 µm, Table 1) was aligned just beneath the oolemma (Figs. 1j, 2c).

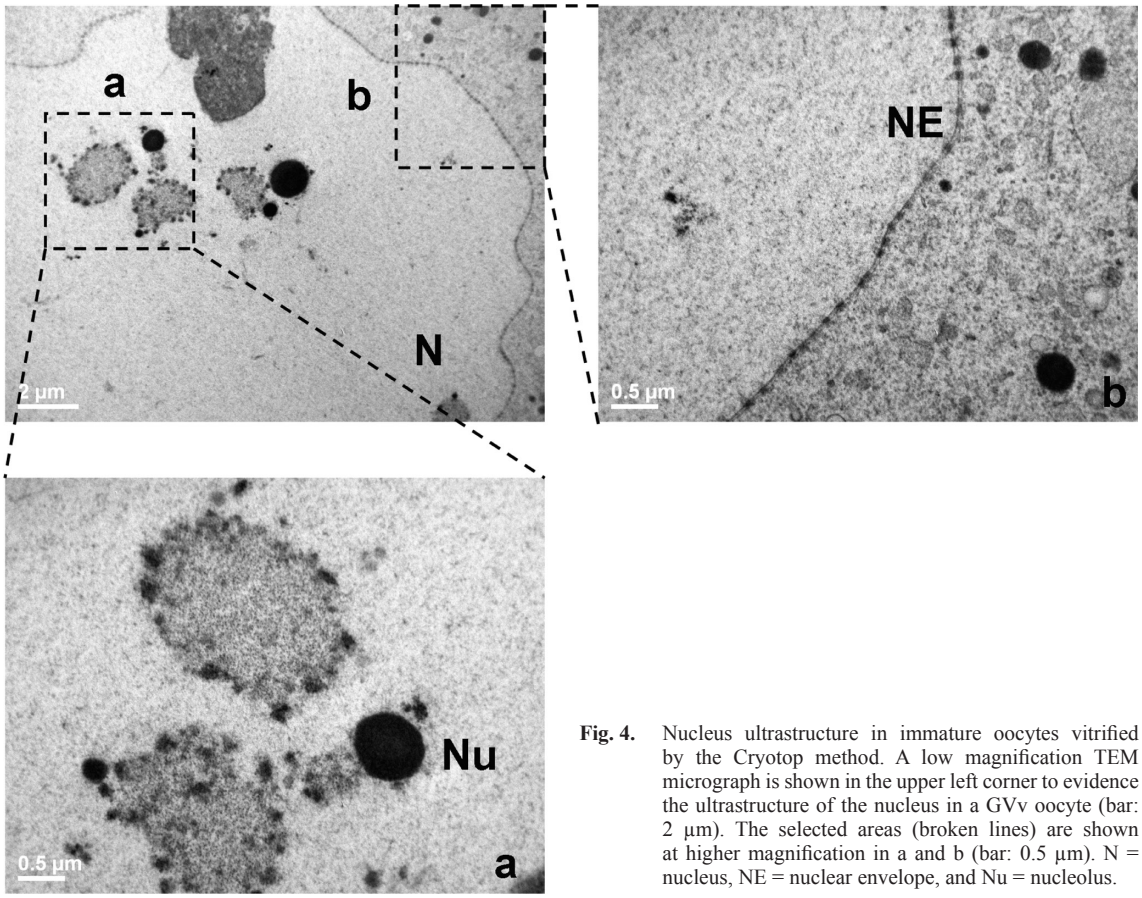

Fig. 4. Nucleus ultrastructure in immature oocytes vitrified by the Cryotop method. A low magnification TEM micrograph is shown in the upper left corner to evidence the ultrastructure of the nucleus in a GVv oocyte (bar: 2 µm). The selected areas (broken lines) are shown at higher magnification in a and b (bar: 0.5 µm). N = nucleus, NE = nuclear envelope, and Nu = nucleolus.

The most abundant organelles were represented by round or ovoid mitochondria (medium diameter ± SD: 0.368 ± 0.084 µm, Table 1), which often associated with numerous elements of SER to form large M-SER aggregates (Fig. 3c). Small MV complexes were found in the ooplasm (Figs. 3c, inset).

Vacuoles bigger than 1.5 µm were rarely observed, as were smaller electron-lucent vacuoles (medium diameter ± SD: 0.686 ± 0.745 µm, Table 1) enclosed by a continuous membrane (Fig. 2c).

Vitrified-warmed MII (MIIv): PCM revealed the extruded PB1 (Fig. 1k). None of the MIIv oocytes differed significantly from the controls, presenting a round shape, a continuous ZP, a thin PVS and an intact oolemma. The cytoplasmic organelle density was high, as seen by LM (Fig. 1l). Low magnification TEM micrographs revealed that organelles were mainly represented by mitochondria and SER membranes (Fig. 1m).

Two different microvillar pattern distributions were observed among oocytes. An abnormal one (30% of MIIv) characterized by a flat oolemma, with a few tufts of blunt and squat microvilli, and another one (70% of MIIv) showing a normal aspect of the microvillar layer, with several long and thin microvilli protruding into the PVS (Fig. 2d), as in fresh mature controls (Fig 2c). At higher magnification, the microvillar membrane was continuous and electron dense (Fig. 2d, inset).

Dark (electron dense) or light forms of spherical CGs (medium diameter ± SD: 0.341 ± 0.065 µm, Table 1) were localized in the cortical region, and only a few were still scattered in the ooplasm. The physiological distribution of CGs aligned under the oolemma was not well preserved after warming, since the CG layer was frequently discontinuous, thus evidencing areas with granule rarefactions and a decreased electron density in all MIIv oocytes (Figs. 1m, 2d).

High-magnification electron micrographs showed round or slightly ovoid mitochondria (medium diameter ± SD: 0.359 ± 0.084 µm, Table 1) with well preserved *cristae* and, sometimes, with clear vesicles included in the matrix.

Similar to what was observed in MIIc oocytes, anastomosing SER tubules were often found in association with mitochondria, forming M-SER aggregates (Fig. 3d, inset). These structures, however, appeared smaller than in MIIc oocytes. MV complexes were instead evenly observed in MIIv oocytes and often present in clusters (Fig. 3d).

Sporadic large vacuoles (medium diameter ± SD: 1.086 ± 1.049 µm, Table 1) were distributed in the ooplasm of most of MIIv oocytes (70%), particularly in the cortical area (Figs. 1l, 1m). In many of these vacuoles, the membrane was discontinuous. In some cases, it was possible to detect cellular debris inside the vacuoles. Vacuoles were most frequently associated with alterations in microvillar and CG patterns and more rarely with smaller M-SER aggregates in the same oocyte. Occasionally, "ooplasmic pouches" were visible in favorable sections, showing a cavity lined by microvilli and CGs (Fig. 5).

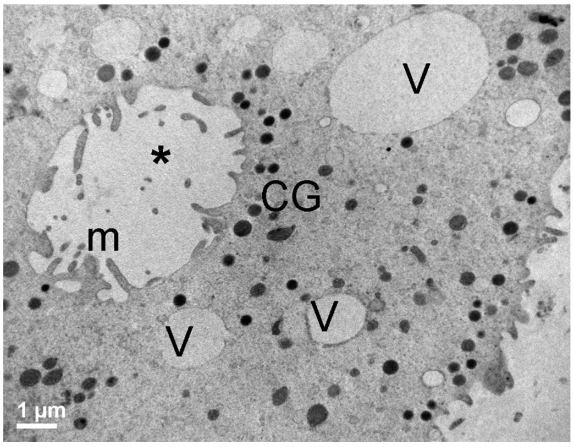

Fig. 5. Ooplasmic pouch in mature human oocytes vitrified by the Cryotop method. An "ooplasmic pouch" (*) in a MIIv oocyte, as seen by TEM. Note the presence of microvilli (m) in the inner vesicular membrane and of several cortical granules (CG) around it. V = vacuoles. Bar: 1 µm.

Discussion

Following vitrification and warming with the Cryotop method [21], immature and mature human oocytes showed a good clinical outcome, as evidenced by the high percentages of survival obtained. These data confirmed the high efficacy of Cryotop method, as already demonstrated in human [11, 26], bovine [27] and sheep [28] oocytes.

LM analysis revealed overall good preservation in all the vitrified-warmed samples, as shown by their rounded shape, homogeneous ooplasm, continuous ZP and narrow PVS and by the presence of an intact nucleus in immature oocytes. TEM analysis showed a physiological distribution of mitochondria, SER and Golgi complexes in GV and MII oocytes after vitrification (GVv and MIIv). These general features coincided with those shown by fresh controls (GVc and MIIc) [1, 16, 23–25, 29, 30]. However, organelle-specific differences between the two maturational stages and between fresh and vitrified oocytes were observed. These differences mainly involved microvilli, CGs, functional associations such as M-SER aggregates and vacuoles.

Microvilli were found to be sensitive to cryodamage in all the stages, since alterations in shape and distribution were clearly observed in part of the vitrified-warmed oocytes. In fact, different from fresh controls, 40% of the immature vitrified-warmed (GVv) oocytes showed the presence of short and small microvilli irregularly spread on the ooplasm surface. In mature vitrified-warmed (MIIv) oocytes, an abnormal microvillar pattern, characterized by the presence of tufts of blunt and squat microvilli, was also found in 30% of the observed samples. The shortening and rarefaction of microvilli could be a consequence of the two cryoprotectants adopted, EG and DMSO, as hypothesized in humans [29–31] and other mammals [32, 33]. It could also be argued that the microvillus shape could be a consequence of the different microtubule and microfilament distributions in the ooplasm, which were evenly distributed in immature oocytes and more cortically located in mature oocytes, for maintenance of CG translocation after GV breakdown [34, 35]. Interestingly, a similar stage-dependent microvillar configuration was described in fresh human oocytes retrieved from a patient with polycystic ovarian syndrome. In this paper, a few microvilli were found at GV stage, while after IVM, at MI-stage their number and size increased to then decrease at MII-stage [36]. However, since full up-to-date full information about the microvillar pattern (shape, length and distribution) during oocyte maturation and subsequent cryopreservation is lacking [1], we can only hypothesize that, even in presence of a possible normal distribution of microvilli, the microvillar layer of GV oocytes−and to a lesser extent of MII oocytes−could be very sensitive to vitrification/warming procedures.

During oocyte maturation, CGs migrate towards the periphery and are ultimately distributes under the oolemma at the MII-stage [37]. In our observations, in both fresh and vitrified-warmed immature GV-stage oocytes, CGs were normally found scattered in the ooplasm. In MII, CGs were generally aligned just beneath the oolemma only in fresh controls (MIIc), since after vitrification, rims of CGs resulted often interrupted. Moreover, a variability in CG electrondensity (ranging from light to dark) was revealed after vitrification, particularly in mature (MIIv) oocytes. Typical CGs are dark electron-dense structures, whereas light scarcely electron-dense CGs can be interpreted as immature organelles or as an early morphological sign of an incoming degranulation (exocytosis) [22–24, 29, 30]. It is known that CGs are Golgi-derived membrane-bound organelles and are involved in the blockage of polispermy [38, 39]. Reduction of their number and variations in electron-density or intracellular localization represent important parameters for evaluation of the quality of a cryopreservation protocol [1]. The amount of dark granules in our vitrified GV oocytes (GVv) seemed to be higher that in their light counterpart, which is different from what was described in frozen-thawed GV oocytes [37]. This may suggest a more advantageous cryopreservation of immature oocytes following Cryotop vitrification.

In the group of vitrified-warmed MII oocytes (MIIv oocytes), a discontinuity in CG stratification was observed, and this was different from the case of MIIc oocytes. Our results are in agreement with the data on human frozen-thawed oocytes [22, 23, 29] and vitrified-warmed oocytes [30]. Analogously to what observed following Cryoleaf and Cryoloop vitrification, the discontinuity of CGs in the sub-oolemmal area of MII oocytes, which is also associated with a heterogeneity in electrondensity, could be a consequence of the vitrification process [30]. This could facilitate a premature granule exocytosis and a subsequent *zona* hardening [40]. The alteration in CG pattern after vitrification has been studied extensively also in mammals. In agreement with our results, a decreased number or abnormal distribution of CGs in pigs [41], sometimes associated with a rupture in dogs [42] and formation of clusters in bovines [27], was observed following cryopreservation.

Mitochondria appeared well preserved through all developmental stages, before and after vitrification [43], since they showed morphological features such as the presence of few arch-like or transverse cristae or the presence of clear vesicles [22, 44]. The presence of functional associations between mitochondria and small vesicles (MV complexes) was commonly observed in all oocytes as well. MV complexes often appeared in clusters in the cortical

and subcortical ooplasm. On the other hand, M-SER aggregates were only found in mature oocytes. By analyzing the trend of MV complexes and M-SER aggregates in our samples, it was possible to speculate that MV complexes are peculiar forms of associations in GV- and MII-stage oocytes with or without vitrification [24, 43, 45]. The presence of isolated SER tubules, and/or underdeveloped SER aggregates, and the virtual absence of M-SER aggregates in GV oocytes, both fresh and vitrified-warmed, could probably be justified as functional immaturity. It is possible that at the GV-stage, there is no need for such a close connection between mitochondria and SER, which is involved in the regulation of intracellular Ca^{2+} sequestration/release [46], because at GV stage the intracellular Ca^{2+} concentration is lower than at the MII stage [47]. On the other hand, fresh mature MII oocytes showed the presence of large M-SER aggregates. These aggregates could contribute to the generation of the typical Ca^{2+} oscillations induced by the fertilizing spermatozoon and could be interpreted by the mature oocyte as a trigger for the fertilization process [23]. This is corroborated by the increase in parthenogenetic activation without sperm penetration shown in vitrified-warmed mature oocytes, probably after a rise in Ca^{2+} level [48]. Morphologically, the reduced dimensions and complexity of the M-SER aggregates that we observed in vitrified-thawed mature MII oocytes could be indicative of possible cryodamage [30].

SER tubules, isolated or interconnected, and MV complexes could both give rise to M-SER aggregates when an oocyte resumes maturation, according to the biochemical needs of the cell. In relation to this, the changes occurring in the oocyte during aging or after prolonged culture confirm the high morphodynamic profile of these organelle associations. In fact, numerous and abnormally large MV complexes are frequently detected in oocytes that have matured *in vitro* or have been kept *in vitro* for a long time [16, 31, 45], suggesting a further remodelling of small MV complexes and/or large M-SER aggregates under these culture conditions.

It is well known that oocyte vacuoles are organelles related to the effect of cryodamage [22, 29, 30]. In fact, using both slow-freezing and vitrification protocols, various degrees of cytoplasmic vacuolization have been reported in human [1, 16, 26, 29, 30, 49] and other mammalian [28, 32, 40] oocytes. Our results showed that in all GV oocytes, irrespective of vitrification, a physiological distribution of small membrane-bound vacuoles was present around the nucleus. However, in 50% of them, minute electron-lucent vacuoles were abnormally located in the cytoplasmic periphery. On the other hand, the presence of isolated large vacuoles distributed in the cortical area, rare at GV stage, increased in MII-stage oocytes following vitrification, affecting 70% of the oocytes. Overall, excessive oocyte vacuolization, irrespective of the maturative stage, was found, thus possibly evidencing signs of cryoinjuries.

These data are in agreement with a previous paper showing [26] evident vacuolization in human MII oocytes vitrified by means of closed Cryotip and open Cryotop devices. The vacuolization was more severe when using the closed procedure. Analogously, other authors [49] found a significantly higher number of vacuoles by using Cryotip device, respect to what found in fresh oocytes. On the other hand, in human MII oocytes vitrified using Cryoloop and Cryoleaf open devices, vacuoles were rarely observed [30]. The above findings open an interesting question concerning a possible cryodevice-dependent vacuolization, perhaps associated with the skill of the operator. Moreover, the different methodologies used to count and measure vacuoles can also make the results variable. Vacuoles are indeed considered the morphological expression of a degenerative process [1, 49] because of their recurrent association with multivesicular bodies and lysosomes [22, 30]. The origin of vacuoles is controversial. Multiple vacuoles in the ooplasm of human oocytes may be caused by swelling and the coalescence of isolated SER membranes or by a mechanism of fusion of pre-existing vesicles from SER or Golgi complexes [50, 51]. Besides, fluid-filled vacuoles are hypothesized to originate from oolemma invaginations, as reported by Van Blerkom [52]. However, larger vacuoles should be morphologically differentiated from the "ooplasmic pouches" that we occasionally observed, which were clearly made by oolemmal invaginations, as evidenced by the presence of several microvilli in the inner side of the membrane and by associated CGs. Since the presence of vacuoles in human mature oocytes might ultimately lead to impairment of oocyte competence for fertilization and/or impaired embryo development [50], low levels of vacuolization in vitrified-warmed oocytes could be considered a marker of good quality oocytes [30].

The ultrastructure of the nucleus at the GV stage was not affected by the eventual cryodamage after Cryotop vitrification, as demonstrated by the good preservation of the nuclear envelopes and subnuclear structures, which were comparable to those of fresh immature oocytes [45, 46, 53].

This study, indeed, demonstrated that even if the Cryotop method allowed good overall preservation of both immature and mature oocytes, it could not avoid the occurrence of peculiar ultrastructural damage. However, the proper CG density and CG localization in the deeper ooplasm (not associated with evident ultrastructural modifications, as demonstrated here) of GVv oocytes make these cellular structures not susceptible to the major cryopreservation-induced injuries in the MII stage, like decreased density, premature CG exocytosis, inward displacement and discontinuity in the subplasmalemmal configuration [22, 29, 30, 49]. The finding that the nuclear ultrastructure was well preserved makes our results of interest, since cryodamage connected to meiosis resumption (i.e., the disappearance of the protective nuclear envelope and the presence of condensed chromosomes maintained by a very cryosensitive meiotic spindle) could be avoided. Finally, the virtual absence of M-SER aggregates at GV stage is another aspect that should be taken into account, since cryopreservation can modify their morpho-functionality, thus altering Ca^{2+} signalling and developmental potential [25, 46, 49, 54].

Even if some reports demonstrated a lower resistance of GV stage oocytes to low temperatures (as measured by survival) [55–57], our ultrastructural results indicate that the oocyte ability to maintain or restore its competence may be better when vitrified at GV-stage. This reinforces the previous morphological data evidencing a better cytoskeletal organization and competence to develop up to blastocyst stage [58]. However, the presence of microvillar alterations and vacuolization in both GV- and MII-stage oocytes deserves further investigation.

The cryopreservation of GV oocytes by vitrification offers attractive perspectives [59], since the resulting GV oocytes represent an important pool of germ cells for women undergoing unstimulated

IVM cycles or at risk of infertility due to ovarian hyperstimulation syndrome or polycystic ovarian syndrome, particularly in those who are poor responders to gonadotropin stimulation [60] or in the case of cancer [61]. Rescue of immature oocytes can also be performed in an IVF cycle when a conventional protocol fails to produce mature oocytes. The optimization of a protocol allowing for retrieval of immature oocytes that can be matured *in vitro* and then successfully vitrified would offer a significant opportunity to preserve fertility [62].

Acknowledgments

Funds for this work were provided by the University La Sapienza (university and faculty grants), by the Department of Life, Health and Environmental Sciences, University of L'Aquila, and by the RAPRUI.

The authors wish to acknowledge Mr. E Battaglione of the Laboratory for Electron Microscopy "Pietro M Motta," Department of Anatomy, Histology, Forensic Medicine and Orthopaedics, University La Sapienza, Rome, and Dr M Giammatteo of the Centre of Microscopy, University of L'Aquila, L'Aquila, Italy. The authors would also thank Prof M Silvia Marottoli for her careful revision of the English language of the manuscript.

Dr E Di Marco, Department of Life, Health and Environmental Sciences, University of L'Aquila, contributed to the electron microscopy preparations and sectioning during her PhD course.

References

1. **Khalili MA, Maione M, Palmerini MG, Bianchi S, Macchiarelli G, Nottola SA.** Ultrastructure of human mature oocytes after vitrification. *Eur J Histochem* 2012; **56**: e38. [Medline] [CrossRef]
2. **Mukaida T, Oka C.** Vitrification of oocytes, embryos and blastocysts. *Best Pract Res Clin Obstet Gynaecol* 2012; **26**: 789–803. [Medline] [CrossRef]
3. **Chian RC, Huang JY, Tan SL, Lucena E, Saa A, Rojas A, Ruvalcaba Castellón LA, García Amador MI, Montoya Sarmiento JE.** Obstetric and perinatal outcome in 200 infants conceived from vitrified oocytes. *Reprod Biomed Online* 2008; **16**: 608–610. [Medline] [CrossRef]
4. **Cobo A, Kuwayama M, Pérez S, Ruiz A, Pellicer A, Remohí J.** Comparison of concomitant outcome achieved with fresh and cryopreserved donor oocytes vitrified by the Cryotop method. *Fertil Steril* 2008; **89**: 1657–1664. [Medline] [CrossRef]
5. **Cobo A, Diaz C.** Clinical application of oocyte vitrification: a systematic review and meta-analysis of randomized controlled trials. *Fertil Steril* 2011; **96**: 277–285. [Medline] [CrossRef]
6. **Herrero L, Martínez M, Garcia-Velasco JA.** Current status of human oocyte and embryo cryopreservation. *Curr Opin Obstet Gynecol* 2011; **23**: 245–250. [Medline]
7. **Zhang Z, Liu Y, Xing Q, Zhou P, Cao Y.** Cryopreservation of human failed-matured oocytes followed by *in vitro* maturation: vitrification is superior to the slow freezing method. *Reprod Biol Endocrinol* 2011; **9**: 156. [Medline] [CrossRef]
8. **Cao YX, Xing Q, Li L, Cong L, Zhang ZG, Wei ZL, Zhou P.** Comparison of survival and embryonic development in human oocytes cryopreserved by slow-freezing and vitrification. *Fertil Steril* 2009; **92**: 1306–1311. [Medline] [CrossRef]
9. **Martínez-Burgos M, Herrero L, Megías D, Salvanes R, Montoya MC, Cobo AC, Garcia-Velasco JA.** Vitrification versus slow freezing of oocytes: effects on morphologic appearance, meiotic spindle configuration, and DNA damage. *Fertil Steril* 2011; **95**: 374–377. [Medline] [CrossRef]
10. **Coticchio G, Bromfield JJ, Sciajno R, Gambardella A, Scaravelli G, Borini A, Albertini DF.** Vitrification may increase the rate of chromosome misalignment in the metaphase II spindle of human mature oocytes. *Reprod Biomed Online* 2009; **19**(Suppl 3): 29–34. [Medline] [CrossRef]
11. **Rienzi L, Romano S, Albricci L, Maggiulli R, Capalbo A, Baroni E, Colamaria S, Sapienza F, Ubaldi F.** Embryo development of fresh *'versus'* vitrified metaphase II oocytes after ICSI: a prospective randomized sibling-oocyte study. *Hum Reprod* 2010; **25**: 66–73. [Medline] [CrossRef]
12. **Smith GD, Serafini PC, Fioravanti J, Yadid I, Coslovsky M, Hassun P, Alegretti JR, Motta EL.** Prospective randomized comparison of human oocyte cryopreservation with slow-rate freezing or vitrification. *Fertil Steril* 2010; **94**: 2088–2095. [Medline] [CrossRef]
13. **Cobo A, Romero JL, Pérez S, de los Santos MJ, Meseguer M, Remohí J.** Storage of human oocytes in the vapor phase of nitrogen. *Fertil Steril* 2010; **94**: 1903–1907. [Medline] [CrossRef]
14. **Parmegiani L, Cognigni GE, Bernardi S, Cuomo S, Ciampaglia W, Infante FE, Tabarelli de Fatis C, Arnone A, Maccarini AM, Filicori M.** Efficiency of aseptic open vitrification and hermetical cryostorage of human oocytes. *Reprod Biomed Online* 2011; **23**: 505–512. [Medline] [CrossRef]
15. **Borini A, Bianchi V.** Cryopreservation of mature and immature oocytes. *Clin Obstet Gynecol* 2010; **53**: 763–774. [Medline] [CrossRef]
16. **Shahedi A, Hosseini A, Khalili MA, Norouzian M, Salehi M, Piriaei A, Nottola SA.** The effect of vitrification on ultrastructure of human *in vitro* matured germinal vesicle oocytes. *Eur J Obstet Gynecol Reprod Biol* 2013; **167**: 69–75. [Medline] [CrossRef]
17. **Coticchio G, Rossi G, Borini A, Grøndahl C, Macchiarelli G, Flamigni C, Fleming S, Cecconi S.** Mouse oocyte meiotic resumption and polar body extrusion *in vitro* are differentially influenced by FSH, epidermal growth factor and meiosis-activating sterol. *Hum Reprod* 2004; **19**: 2913–2918. [Medline] [CrossRef]
18. **Nottola SA, Heyn R, Camboni A, Correr S, Macchiarelli G.** Ultrastructural characteristics of human granulosa cells in a coculture system for *in vitro* fertilization. *Microsc Res Tech* 2006; **69**: 508–516. [Medline] [CrossRef]
19. **Rossi G, Macchiarelli G, Palmerini MG, Canipari R, Cecconi S.** Meiotic spindle configuration is differentially influenced by FSH and epidermal growth factor during *in vitro* maturation of mouse oocytes. *Hum Reprod* 2006; **21**: 1765–1770. [Medline] [CrossRef]
20. **Fasano G, Demeestere I, Englert Y.** *In-vitro* maturation of human oocytes: before or after vitrification? *J Assist Reprod Genet* 2012; **29**: 507–512. [Medline] [CrossRef]
21. **Antinori M, Licata E, Dani G, Cerusico F, Versaci C, Antinori S.** Cryotop vitrification of human oocytes results in high survival rate and healthy deliveries. *Reprod Biomed Online* 2007; **14**: 72–79. Erratum in: Reprod Biomed Online 2007; 15: 667. dosage error in text. [Medline] [CrossRef]
22. **Nottola SA, Macchiarelli G, Coticchio G, Bianchi S, Cecconi S, De Santis L, Scaravelli G, Flamigni C, Borini A.** Ultrastructure of human mature oocytes after slow cooling cryopreservation using different sucrose concentrations. *Hum Reprod* 2007; **22**: 1123–1133. [Medline] [CrossRef]
23. **Coticchio G, Borini A, Distratis V, Maione M, Scaravelli G, Bianchi V, Macchiarelli G, Nottola SA.** Qualitative and morphometric analysis of the ultrastructure of human oocytes cryopreserved by two alternative slow cooling protocols. *J Assist Reprod Genet* 2010; **27**: 131–140. [Medline] [CrossRef]
24. **Motta PM, Nottola SA, Micara G, Familiari G.** Ultrastructure of human unfertilized oocytes and polyspermic embryos in an IVF-ET program. *Ann N Y Acad Sci* 1988; **541**: 367–383. [Medline] [CrossRef]
25. **Motta PM, Nottola SA, Familiari G, Makabe S, Stallone T, Macchiarelli G.** Morphodynamics of the follicular-luteal complex during early ovarian development and reproductive life. *Int Rev Cytol* 2003; **223**: 177–288. [Medline] [CrossRef]
26. **Bonetti A, Cervi M, Tomei F, Marchini M, Ortolani F, Manno M.** Ultrastructural evaluation of human metaphase II oocytes after vitrification: closed versus open devices. *Fertil Steril* 2011; **95**: 928–935. [Medline] [CrossRef]
27. **Morató R, Izquierdo D, Paramio MT, Mogas T.** Cryotops *versus* open-pulled straws (OPS) as carriers for the cryopreservation of bovine oocytes: effects on spindle and chromosome configuration and embryo development. *Cryobiology* 2008; **57**: 137–141. [Medline] [CrossRef]
28. **Ebrahimi B, Valojerdi MR, Eftekhari-Yazdi P, Baharvand H.** Ultrastructural changes of sheep cumulus-oocyte complexes following different methods of vitrification. *Zygote* 2012; **20**: 103–115. [Medline] [CrossRef]
29. **Nottola SA, Coticchio G, De Santis L, Macchiarelli G, Maione M, Bianchi S, Iaccarino M, Flamigni C, Borini A.** Ultrastructure of human mature oocytes after slow cooling cryopreservation with ethylene glycol. *Reprod Biomed Online* 2008; **17**: 368–377. [Medline] [CrossRef]
30. **Nottola SA, Coticchio G, Sciajno R, Gambardella A, Maione M, Scaravelli G, Bianchi S, Macchiarelli G, Borini A.** Ultrastructural markers of quality in human mature oocytes vitrified using cryoleaf and cryoloop. *Reprod Biomed Online* 2009; **19**(Suppl 3): 17–27. [Medline] [CrossRef]
31. **Sathananthan AH, Trounson AO.** Effects of culture and cryopreservation on human oocyte and embryo ultrastructure and function. *In*: Van Blerkom J, Motta PM (eds) Ultrastructure of Human Gametogenesis and Early Embryogenesis. Kluwer Academic Publishers, Boston; 1989: 181–199.
32. **Wu C, Rui R, Dai J, Zhang C, Ju S, Xie B, Lu X, Zheng X.** Effects of cryopreservation on the developmental competence, ultrastructure and cytoskeletal structure of porcine oocytes. *Mol Reprod Dev* 2006; **73**: 1454–1462. [Medline] [CrossRef]

33. **Boonkusol D, Faisaikarm T, Dinnyes A, Kitiyanant Y.** Effects of vitrification procedures on subsequent development and ultrastructure of *in vitro*-matured swamp buffalo (*Bubalus bubalis*) oocytes. *Reprod Fertil Dev* 2007; **19**: 383–391. [Medline] [CrossRef]
34. **Lee J, Miyano T, Moor RM.** Spindle formation and dynamics of gamma-tubulin and nuclear mitotic apparatus protein distribution during meiosis in pig and mouse oocytes. *Biol Reprod* 2000; **62**: 1184–1192. [Medline] [CrossRef]
35. **Modina S, Beretta M, Lodde V, Lauria A, Luciano AM.** Cytoplasmic changes and developmental competence of bovine oocytes cryopreserved without cumulus cells. *Eur J Histochem* 2004; **48**: 337–346. [Medline]
36. **Yang YJ, Zhang YJ, Li Y**. Ultrastructure of human oocytes of different maturity stages and the alteration during in vitro maturation. *Fertil Steril* 2009; **92**: 396.e1–396.e6. [Medline] [CrossRef]
37. **Ghetler Y, Skutelsky E, Ben Nun I, Ben Dor L, Amihai D, Shalgi R.** Human oocyte cryopreservation and the fate of cortical granules. *Fertil Steril* 2006; **86**: 210–216. [Medline] [CrossRef]
38. **Sathananthan AH, Trounson AO.** Ultrastructural observations on cortical granules in human follicular oocytes cultured *in vitro*. *Gamete Res* 1982; **5**: 191–198. [CrossRef]
39. **Familiari G, Heyn R, Relucenti M, Nottola SA, Sathananthan AH.** Ultrastructural dynamics of human reproduction, from ovulation to fertilization and early embryo development. *Int Rev Cytol* 2006; **249**: 53–141. [Medline] [CrossRef]
40. **Hyttel P, Vajta G, Callesen H.** Vitrification of bovine oocytes with the open pulled straw method: ultrastructural consequences. *Mol Reprod Dev* 2000; **56**: 80–88. [Medline] [CrossRef]
41. **Marco-Jiménez F, Casares-Crespo L, Vicente JS.** Effect of cytochalasin B pre-treatment of *in vitro* matured porcine oocytes before vitrification. *Cryo Lett* 2012; **33**: 24–30. [Medline]
42. **Turathum B, Saikhun K, Sangsuwan P, Kitiyanant Y.** Effects of vitrification on nuclear maturation, ultrastructural changes and gene expression of canine oocytes. *Reprod Biol Endocrinol* 2010; **8**: 70. [Medline] [CrossRef]
43. **Motta PM, Nottola SA, Makabe S, Heyn R.** Mitochondrial morphology in human fetal and adult female germ cells. *Hum Reprod* 2000; **15**(Suppl 2): 129–147. [Medline] [CrossRef]
44. **Sathananthan AH, Selvaraj K, Girijashankar ML, Ganesh V, Selvaraj P, Trounson AO.** From oogonia to mature oocytes: inactivation of the maternal centrosome in humans. *Microsc Res Tech* 2006; **69**: 396–407. [Medline] [CrossRef]
45. **El Shafie M, Sousa M, Windt M-L, Kruger TF.** An Atlas of the Ultrastructure of Human Oocytes. Parthenon Publishing, New York, USA, 2000.
46. **Makabe S, Van Blerkom J, Nottola SA, Naguro T.** Atlas of Human Female Reproductive Function. Ovarian Development to Early Embryogenesis after *In Vitro* Fertilization. Taylor and Francis, London, UK; 2006: 180.
47. **Zhou HM, Jin SY.** Ca2+ cascade and meiotic resumption of the caprine primary oocyte. *Reprod Domest Anim* 2007; **42**: 555–559. [Medline] [CrossRef]
48. **Somfai T, Ozawa M, Noguchi J, Kaneko H, Kuriani Karja NW, Farhudin M, Dinnyés A, Nagai T, Kikuchi K.** Developmental competence of *in vitro*-fertilized porcine oocytes after *in vitro* maturation and solid surface vitrification: effect of cryopreservation on oocyte antioxidative system and cell cycle stage. *Cryobiology* 2007; **55**: 115–126. [Medline] [CrossRef]
49. **Gualtieri R, Mollo V, Barbato V, Fiorentino I, Iaccarino M, Talevi R.** Ultrastructure and intracellular calcium response during activation in vitrified and slow-frozen human oocytes. *Hum Reprod* 2011; **26**: 2452–2460. [Medline] [CrossRef]
50. **Ebner T, Moser M, Sommergruber M, Gaiswinkler U, Shebl O, Jesacher K, Tews G.** Occurrence and developmental consequences of vacuoles throughout preimplantation development. *Fertil Steril* 2005; **83**: 1635–1640. [Medline] [CrossRef]
51. **Otsuki J, Okada A, Morimoto K, Nagai Y, Kubo H.** The relationship between pregnancy outcome and smooth endoplasmic reticulum clusters in MII human oocytes. *Hum Reprod* 2004; **19**: 1591–1597. [Medline] [CrossRef]
52. **Van Blerkom J.** Occurrence and developmental consequences of aberrant cellular organization in meiotically mature human oocytes after exogenous ovarian hyperstimulation. *J Electron Microsc Tech* 1990; **16**: 324–346. [Medline] [CrossRef]
53. **Miyara F, Migne C, Dumont-Hassan M, Le Meur A, Cohen-Bacrie P, Aubriot FX, Glissant A, Nathan C, Douard S, Stanovici A, Debey P.** Chromatin configuration and transcriptional control in human and mouse oocytes. *Mol Reprod Dev* 2003; **64**: 458–470. [Medline] [CrossRef]
54. **Nikiforaki D, Vanden Meerschaut F, Qian C, De Croo I, Lu Y, Deroo T, Van den Abbeel E, Heindryckx B, De Sutter P.** Oocyte cryopreservation and *in vitro* culture affect calcium signalling during human fertilization. *Hum Reprod* 2014; **29**: 29–40. [Medline] [CrossRef]
55. **Cao YX, Chian RC.** Fertility preservation with immature and *in vitro* matured oocytes. *Semin Reprod Med* 2009; **27**: 456–464. [Medline] [CrossRef]
56. **Imesch P, Scheiner D, Xie M, Fink D, Macas E, Dubey R, Imthurn B.** Developmental potential of human oocytes matured *in vitro* followed by vitrification and activation. *J Ovarian Res* 2013; **6**: 30. [Medline] [CrossRef]
57. **Lee JA, Barritt J, Moschini RM, Slifkin RE, Copperman AB.** Optimizing human oocyte cryopreservation for fertility preservation patients: should we mature then freeze or freeze then mature? *Fertil Steril* 2013; **99**: 1356–1362. [Medline] [CrossRef]
58. **Egerszegi I, Somfai T, Nakai M, Tanihara F, Noguchi J, Kaneko H, Nagai T, Rátky J, Kikuchi K.** Comparison of cytoskeletal integrity, fertilization and developmental competence of oocytes vitrified before or after *in vitro* maturation in a porcine model. *Cryobiology* 2013; **67**: 287–292. [Medline] [CrossRef]
59. **Fasano G, Moffa F, Dechène J, Englert Y, Demeestere I.** Vitrification of *in vitro* matured oocytes collected from antral follicles at the time of ovarian tissue cryopreservation. *Reprod Biol Endocrinol* 2011; **9**: 150. [Medline] [CrossRef]
60. **Barton SE, Missmer SA, Berry KF, Ginsburg ES.** Female cancer survivors are low responders and have reduced success compared with other patients undergoing assisted reproductive technologies. *Fertil Steril* 2012; **97**: 381–386. [Medline] [CrossRef]
61. **Gulekli B, Kovali M, Aydiner F, Dogan S, Dogan SS.** IVM is an alternative for patients with PCO after failed conventional IVF attempt. *J Assist Reprod Genet* 2011; **28**: 495–499. [Medline] [CrossRef]
62. **Fadini R, Mignini Renzini M, Dal Canto M, Epis A, Crippa M, Caliari I, Brigante C, Coticchio G.** Oocyte *in vitro* maturation in normo-ovulatory women. *Fertil Steril* 2013; **99**: 1162–1169. [Medline] [CrossRef]